

PROTAC-DB 2.0: an updated database of PROTACs

Gaoqi Weng^{1,2,†}, Xuanyan Cai^{1,3,†}, Dongsheng Cao⁴, Hongyan Du¹, Chao Shen¹, Yafeng Deng², Qiaojun He^{1,3}, Bo Yang¹, Dan Li^{1,*} and Tingjun Hou^{1,*}

¹Innovation Institute for Artificial Intelligence in Medicine of Zhejiang University, College of Pharmaceutical Sciences, Zhejiang University, Hangzhou 310058, Zhejiang, China, ²CarbonSilicon AI Technology Co., Ltd, Hangzhou 310018, Zhejiang, China, ³Center for Drug Safety Evaluation and Research, Zhejiang Province Key Laboratory of Anti-Cancer Drug Research, College of Pharmaceutical Sciences, Zhejiang University, Hangzhou 310058, Zhejiang, China and ⁴Xiangya School of Pharmaceutical Sciences, Central South University, Changsha 410004, Hunan, China

Received August 29, 2022; Revised September 23, 2022; Editorial Decision October 07, 2022; Accepted October 11, 2022

ABSTRACT

Proteolysis targeting chimeras (PROTACs), which harness the ubiquitin-proteasome system to selectively induce targeted protein degradation, represent an emerging therapeutic technology with the potential to modulate traditional undruggable targets. Over the past few years, this technology has moved from academia to industry and more than 10 PROTACs have been advanced into clinical trials. However, designing potent PROTACs with desirable drug-like properties still remains a great challenge. Here, we report an updated online database, PROTAC-DB 2.0, which is a repository of structural and experimental data about PROTACs. In this 2nd release, we expanded the number of PROTACs to 3270, which corresponds to a 96% expansion over the first version. Meanwhile, the numbers of warheads (small molecules targeting the proteins of interest), linkers, and E3 ligands (small molecules recruiting E3 ligases) have increased to over 360, 1500 and 80, respectively. In addition, given the importance and the limited number of the crystal target-PROTAC-E3 ternary complex structures, we provide the predicted ternary complex structures for PROTACs with good degradation capability using our PROTAC-Model method. To further facilitate the analysis of PROTAC data, a new filtering strategy based on the E3 ligases is also added. PROTAC-DB 2.0 is available online at <http://cadd.zju.edu.cn/protacdb/>.

INTRODUCTION

In the past few years, selective targeted protein degradation with the proteolysis targeting chimera (PROTAC) strategy represents an emerging therapeutic approach and has drawn

substantial interest in the pharmaceutical field (1–4). PROTACs are heterobifunctional small molecules, typically consisting of two small molecules conjugated by a linker: one small molecule targets the protein of interest (warhead) and the other is capable of recruiting an E3 ligase (E3 ligand). Unlike traditional small-inhibitor-mediated pharmacology, PROTACs induce the ubiquitylation and the subsequent proteasomal degradation process of target proteins with the catalytic-type mechanism, which only requires transient binding to the proteins of interest (5,6). Furthermore, PROTACs have the potential to extend druggable space to targets with shallow and broad active sites, which are previously considered intractable or undruggable (4,6).

Since the first peptide-based PROTAC was reported by Sakamoto *et al.* (1), the PROTAC technology has been successfully applied to the degradation of >200 target proteins (7). Besides, a number of PROTACs show highly potent and specific protein degradation capability in cellular assays and even *in vivo* (5,8–15). For example, in 2019, Bai *et al.* developed SD-36, an efficacious and selective small molecule PROTAC targeting signal transducer and activator of transcription 3 (STAT3), which has historically been considered as an undruggable target (9). SD-36 can induce complete and durable tumor regression in multiple xenograft mouse models. In 2021, the first PROTAC capable of selectively degrading cyclin-dependent kinase 12 (CDK12), BSJ-4-116, was reported by Jiang *et al.*, which showed potent antiproliferative effects and could overcome CDK12^{C1039F} mutation resistant to covalent CDK12 inhibitors (15). Moreover, two PROTACs named ARV-110 and ARV-471, for the treatment of metastatic castration-resistant cancer (NCT03888612) and metastatic ER⁺/HER2⁻ breast cancer (NCT04072952), respectively, have entered phase II trials. In addition, numerous companies have also disclosed projects in preclinical and early clinical development (4).

Despite significant progress achieved, attaining potent PROTACs with suitable absorption, distribution, metabolism and excretion (ADME) properties adequate for

*To whom correspondence should be addressed. Tel: +86 517 8820 8412; Email: tingjunhou@zju.edu.cn

Correspondence may also be addressed to Dan Li. Email: lidancps@zju.edu.cn

†The authors wish it to be known that, in their opinion, the first two authors should be regarded as Joint First Authors.

oral dosing still remains a challenge. The high molecular weight of PROTACs brings an elevated level of technical complexity for medicinal chemists to optimize drug-like properties (16,17). In addition, the linker design is associated with the activity, selectivity, and drug-like properties of PROTACs (18). To boost the rational design of PROTACs, we previously developed an online database, PROTAC-DB, which has provided users an easy-to-use resource to query the comprehensive structural information and experimental data about PROTACs since 2020 (7). The diverse information contains the chemical structures, physicochemical properties, and biological activities of PROTACs. Moreover, for better analysis, PROTACs are further split into three domains, including warheads, linkers and E3 ligands. The PROTACs with the consistent warheads, linkers or E3 ligands are summarized in the corresponding detailed information pages. Over the past 2 years, PROTAC-DB has been viewed >63 000 times from >60 countries around the world and has been highly cited by researchers.

Here, we provide an updated database, PROTAC-DB 2.0, whose quantity of existing data has increased enormously. For instance, the number of PROTACs has expanded significantly from 1662 to 3270. In addition, considering the importance of structural data of target-PROTAC-E3 ternary complexes for PROTAC design and the very limited number of their crystal structures, we also integrated the predicted ternary complex models for PROTACs with good degradation capacity using the PROTAC-Model method developed in our group into the database (19). Currently, the number of the predicted ternary complex models is >660. Moreover, for user convenience, a new filtering option based on the E3 ligases was developed to enable the fast and effective analysis of structural information of PROTACs in the database.

MATERIALS AND METHODS

Data collection and processing

Consistent with PROTAC-DB 1.0, literature was curated from PubMed via the keywords of 'degrader* OR protac OR proteolysis targeting chimera'. Then, information regarding the chemical structures as well as the biological activities of PROTACs was manually extracted from the published papers. The biological activities include degradation capacities, cellular activities, and binding affinities. Additionally, we collected the parallel artificial membrane permeability (PAMPA) and Caco-2 permeability data for PROTACs.

For the PROTACs with DC_{50} data, we also collected the corresponding PDB files of the target proteins and E3 ligases from the PDB database. The crystal structures of some target proteins that were not suitable for ternary complex modeling were excluded from the subsequent preprocessing step, such as the androgen receptor which lacks the antagonist-bound crystal structure of the ligand-binding domain (20). In addition, for the PROTACs without a specific E3 ligase or capable of recruiting multiple E3 ligases, we did not conduct structural modeling either, such as inhibitors of apoptosis (IAP) E3 ligases, a family of proteins involved in programmed cell death (21). All structures were preprocessed by the same protocol used by PROTAC-Model (19). First, we corrected the nonstandard residues in

the structures. Then, we processed all structures by the Protein Preparation Wizard (22) module of Schrödinger 2020, including assigning bond orders, removing waters, adding hydrogens, filling in missing side chains, and minimizing the structures with the OPLS.2005 force field. For the crystal structures without small-molecule structures corresponding to the warheads or E3 ligands, Glide (SP) was used for the docking calculation with the default settings (23). Warheads and E3 ligands were processed by the LigPrep program of Schrödinger (*LigPrep*, Schrödinger Release 2020-1). The maximum number of stereoisomers per ligand were set to 4. The location of the cocrystallized ligand in the corresponding structure was set as the docking site.

Modeling of PROTAC-mediated ternary complexes

Both of FRODOCK-based protocol and RosettaDock-based refinement in the PROTAC-Model were utilized to predict the structures of PROTAC-mediated ternary complexes with the default settings (19,24,25). In the FRODOCK-based protocol, the larger protein was set as the receptor protein and the other as the ligand protein. The docking site was centered on the anchor atom for the linker in the ligand of the receptor protein. Then, the generated conformations were screened by four filtering steps, including interface residues filtering, modeling of full PROTAC conformations, evaluation of PROTAC conformations, and assessment of PROTAC binding modes. Afterward, the remaining models were reranked and clustered by VoroMQA (26) and FCC clustering method (27), respectively. Subsequently, RosettaDock was used for the refinement of the best model in each cluster. Similar filtering, reranking, and clustering steps were then executed for the resulting models.

RESULTS

Data overview

Over the past 2 years, the PROTAC field has experienced rapid development. The statistical data of PROTAC-DB is summarized in Table 1. Currently, 3270 PROTACs are archived in the PROTAC-DB 2.0, representing an increase of >96% (1608 PROTACs) since the version 1.0. Meanwhile, the number of warheads has grown from 202 to 365, the number of E3 ligands from 65 to 82, and the number of linkers from 806 to 1501. In addition to the significant expansion of chemical structures, PROTAC-DB 2.0 has also added lots of biological activity data, including DC_{50} data (from 379 to 705), cellular activity data (from 437 to 1095), Western blotting data (from 1144 to 2073), binding affinity data between PROTACs and target proteins (from 411 to 818), PROTACs and E3 ligases (from 130 to 198), for the formation of ternary complexes (from 26 to 54). Regarding protein data, PROTAC-DB 2.0 contains 280 target proteins and 13 E3 ligases. Additionally, the number of the crystal structures of target-PROTAC-E3 ternary complexes has increased from 11 to 18. However, this structural data is still very limited, which would significantly hinder the insight into the structure-activity relationship of PROTACs. Therefore, in PROTAC-DB 2.0, we integrated 664 ternary complex structures predicted by our PROTAC-Model method to help users further rationalize PROTAC

Table 1. Data statistics of PROTAC-DB 1.0 and 2.0

Data category	Version 1.0	Version 2.0
Number of PROTACs	1662	3270
Number of warheads	202	365
Number of E3 ligands	65	82
Number of linkers	806	1501
Number of PROTACs with DC50 data	379	705
Number of PROTACs with cellular activity data	437	1095
Number of PROTACs with Western blotting data	1144	2073
Number of PROTACs with binding affinity data between PROTACs and target proteins	411	818
Number of PROTACs with binding affinity data between PROTACs and E3 ligases	130	198
Number of PROTACs with binding affinity data for the formation of ternary complexes	26	54
Number of target proteins	147	280
Number of E3 ligases	11	13
Number of crystal structures	11	18
Number of predicted structures	/	664
Number of PROTACs with cell permeability data	/	41

design. Moreover, considering the importance of the cell permeability of PROTACs for further clinic usage, we collected their PAMPA and Caco-2 permeability data for a total of 41 PROTACs. This data is displayed in the activity data tab in the detailed information pages of PROTACs.

Target-PROTAC-E3 ternary complex structure display

In order to facilitate users to browse the structures of PROTAC-mediated ternary complexes, we added a ternary complex structure tab to the detailed information pages of PROTACs (Figure 1). 3Dmol.js (28), a WebGL-based molecular viewer, was integrated into the database for molecular visualization. The brief instructions of 3Dmol.js are shown as follows: (i) Rotation: press and hold the left mouse button, (ii) Zoom: use the scroll button and (iii) Translation: press and hold the scroll button. After searching, as shown in Figure 2A, the PROTACs containing the crystal and predicted structures are marked with ‘Crystal’ and ‘Pred’, respectively. Clicking on the compound ID can jump to the detailed information pages and then access the ternary complex structure tab.

For the crystal ternary complex structures (Figure 1A), structures can be interactively displayed in the first row with 3Dmol.js. In the second row, users can choose the structural data for a specific target to display when the structures between this PROTAC and multiple target proteins are solved. The PDB code, the link to the PDB database, and the downloaded file are summarized in the table.

For the predicted ternary complex structures, as shown in Figure 1B, PROTAC-DB 2.0 provides interactive molecular visualization for the top 10 clusters predicted by the FRODOCK-based protocol and RosettaDock-based refinement, respectively, which contain up to three representative conformations each. Similarly, the structures and target options are shown in the first and second rows, respectively.

The upper table contains the display status, the model name, the predicted protocol, the value of the interface energy between the target proteins and E3 ligases, and the downloaded files. For the model name, the first and second numbers represent the best rank from the same cluster and the rank of the model according to the interface energy, respectively. For instance, cluster_1.4.pdb belongs to the cluster 1 and is ranked fourth based on the interface energy. In addition, clicking on the selected row in the table can show the corresponding model on the molecular viewer. The statistics of the predicted structures are summarized in the lower table, including the file name, the number of models, the file size, and the downloaded file. In the file name, the ‘Cluster’ and ‘All’ suffixes represent the generated models after and before clustering, respectively. Since only the top 10 clusters are shown online, the compressed tar files for all predicted models are also available for downloading if users are interested in other generated conformations. Each cluster also only incorporates no more than three conformations.

New filtering functionality based on E3 ligases

The query or browsing results for a specific target protein are shown in Figure 2A, including chemical structures, compound IDs, target proteins, and biological activities. Clicking on the filtering button can open the filtering tool. In addition to the initial filtering options based on the physiochemical properties (e.g. ring count, molecular weight, and heavy atom count), we provide a new filtering mode based on the E3 ligases. As displayed in Figure 2A, for Bromodomain-containing protein 4 (BRD4), researchers develop a number of PROTACs using multiple E3 ligases. Users can choose a class of PROTACs with a specific E3 ligase to display. Moreover, when users retrieve the database using chemical structures, except for the E3 ligases and physiochemical properties, they can further refine the search according to the target proteins.

For the PROTAC tab in the detailed information pages of warheads (Figure 2B), the first row summarizes the warhead structures integrated into PROTACs after modification. The filtering options based on the target proteins and E3 ligases are integrated into the second and third rows, respectively, to facilitate the analysis of the PROTAC data.

CONCLUSION

By virtue of the unique mechanisms and potential advantages over traditional inhibitors, PROTAC technology has attracted extensive attention from the pharmaceutical field. With the continuous efforts of medicinal chemists, this technology has made substantial progress, and the number of PROTACs has increased greatly in recent years. Nevertheless, this technology is still maturing. PROTAC-DB is continually supported to provide comprehensive and reliable information about PROTACs with the aim of helping PROTAC design. In PROTAC-DB 2.0, there are 1608 PROTACs newly added compared with the version 1.0. In addition, to compensate for the limited number of crystal target-PROTAC-E3 ternary complex structures, we added 664 predicted ternary complex structures generated by our PROTAC-Model method. The usability of the web interface is also further improved with the filtering option based

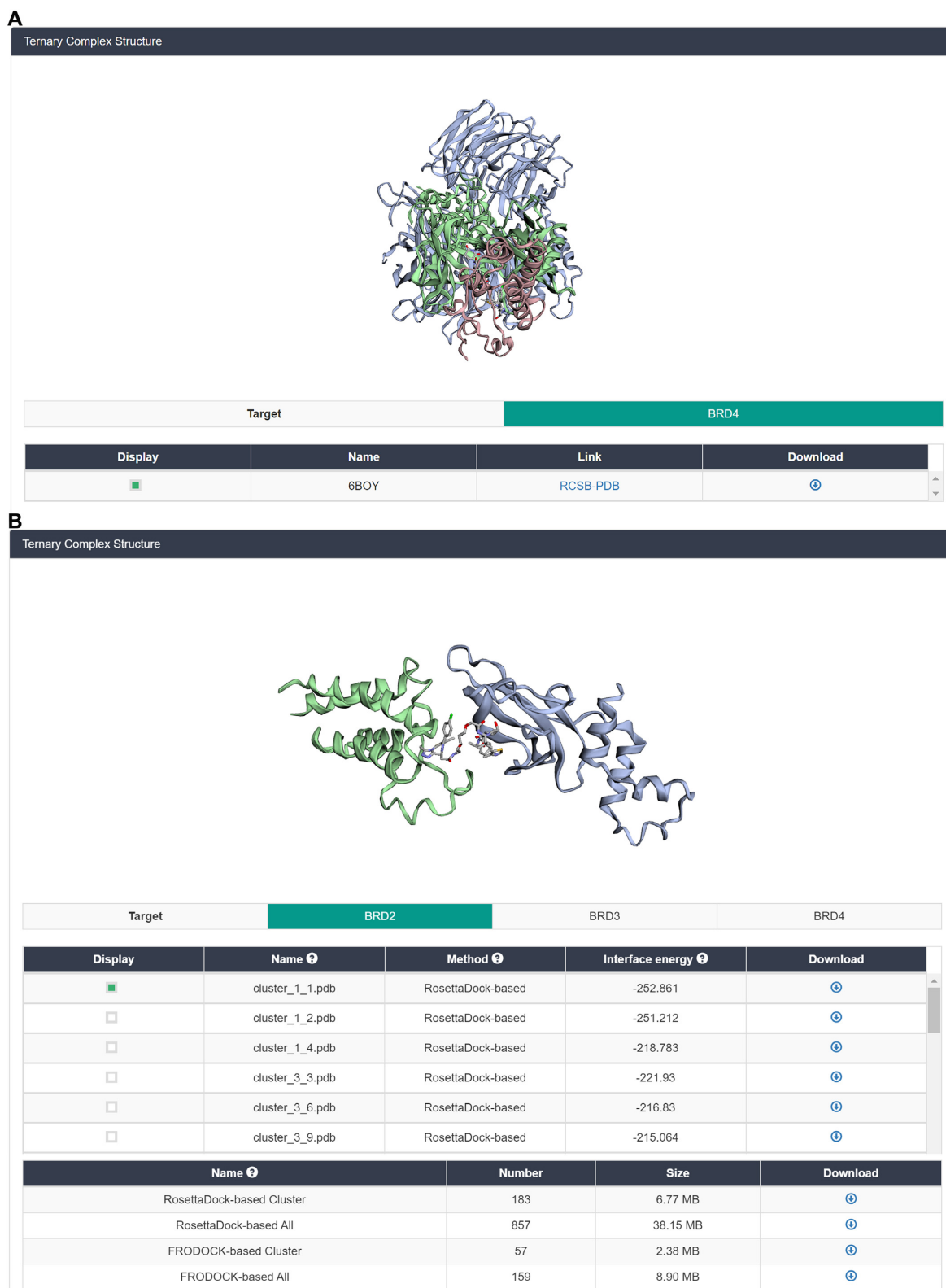


Figure 1. Ternary complex structure tabs for the (A) crystal and (B) predicted structures in the detailed information pages of PROTACs.

A Showing 1 to 50 of 222 entries Per page: 50 Filters 1 2 3 4 5 Next > Last >>

ID/Target	Compound	Degradation		Protac to Target		Protac to E3		Ternary complex		Cellular activities (nM)		
		DC50	Dmax	IC50	Kd	IC50	Kd	IC50	Kd	IC50	EC50	GI50
1784		0.095	96	4.2		613				0.63		
BRD4	(Crystal)	Degradation of BRD4 in PC3-S1 cells after 4 h treatment										
234		0.32										
BRD4	TD-428 (Pred)	Degradation of BRD4 in 22RV1 cells after 24 h treatment										
Eur J Med Chem. 2019 Mar 15;166:65-74												

Filters

Showing 1 to 50 of 222 entries

E3 ligase: All AhR cIAP1 CRBN DCAF16 FEM1B MDM2 RNF114 RNF4 VHL XIAP

Ring Count: 6 To 11 | logP: 0.29 To 8.94 | Polar Area (Å²): 110.94 To 285.5

Molecular Weight: 643.6 To 1201.4 | H Bond Donor Count: 1 To 6 | Rotatable Bond Count: 4 To 37

Heavy Atom Count: 47 To 84 | H Bond Acceptor Count: 7 To 21

Clear Submit

B

PROTAC

Target: All BRD2 BRD2 BD2 BRD3 BRD3 BD1 BRD4 BRD4 BD1

E3 ligase: All AhR cIAP1 CRBN DCAF16 FEM1B MDM2 RNF114 RNF4 VHL XIAP

Showing 1 to 20 of 195 entries Per page: 20 1 2 3 4 5 Next > Last >>

ID/Target	Compound	Degradation		Protac to Target		Protac to E3		Ternary complex		Cellular activities (nM)		
		DC50	Dmax	IC50	Kd	IC50	Kd	IC50	Kd	IC50	EC50	GI50
234		0.32										
BRD4	TD-428 (Pred)	Degradation of BRD4 in 22RV1 cells after 24 h treatment										
Eur J Med Chem. 2019 Mar 15;166:65-74												

Figure 2. The query or browsing results for (A) BRD4 and (B) the PROTAC tab in the detailed information pages of warheads.

on the E3 ligases. With these advancements, we expect that PROTAC-DB 2.0 will provide a better support for the rational design of PROTACs.

FUNDING

National Key Research and Development Program of China [2021YFF1201400]; National Natural Science Foundation of China [22220102001]; Natural Science Foundation of Zhejiang Province [LD22H300001]. Funding for open access charge: Research and Development Program of China.

Conflict of interest statement. None declared.

REFERENCES

- Sakamoto, K.M., Kim, K.B., Kumagai, A., Mercurio, F., Crews, C.M. and Deshaies, R.J. (2001) Protacs: chimeric molecules that target proteins to the Skp1-Cullin-F box complex for ubiquitination and degradation. *Proc. Natl. Acad. Sci. U.S.A.*, **98**, 8554–8559.
- Schneekloth, A.R., Puchault, M., Tae, H.S. and Crews, C.M. (2008) Targeted intracellular protein degradation induced by a small molecule: en route to chemical proteomics. *Bioorg. Med. Chem. Lett.*, **18**, 5904–5908.
- Itoh, Y., Ishikawa, M., Naito, M. and Hashimoto, Y. (2010) Protein knockdown using methyl bestatin–ligand hybrid molecules: design and synthesis of inducers of ubiquitination-mediated degradation of cellular retinoic acid-binding proteins. *J. Am. Chem. Soc.*, **132**, 5820–5826.
- Bekes, M., Langley, D.R. and Crews, C.M. (2022) PROTAC targeted protein degraders: the past is prologue. *Nat. Rev. Drug Discov.*, **21**, 181–200.
- Bondeson, D.P., Mares, A., Smith, I.E.D., Ko, E., Campos, S., Miah, A.H., Mulholland, K.E., Routly, N., Buckley, D.L., Gustafson, J.L. *et al.* (2015) Catalytic in vivo protein knockdown by small-molecule PROTACs. *Nat. Chem. Biol.*, **11**, 611–617.
- Schneider, M., Radoux, C.J., Hercules, A., Ochoa, D., Dunham, I., Zalmas, L.P., Hessler, G., Ruf, S., Shanmugasundaram, V., Hann, M.M. *et al.* (2021) The PROTACtable genome. *Nat. Rev. Drug Discov.*, **20**, 789–797.
- Weng, G., Shen, C., Cao, D., Gao, J., Dong, X., He, Q., Yang, B., Li, D., Wu, J. and Hou, T. (2021) PROTAC-DB: an online database of PROTACs. *Nucleic Acids Res.*, **49**, D1381–D1387.
- Winter, G.E., Buckley, D.L., Paulk, J., Roberts, J.M., Souza, A., Dhe-Paganon, S. and Bradner, J.E. (2015) Phthalimide conjugation as a strategy for in vivo target protein degradation. *Science*, **348**, 1376–1381.
- Bai, L., Zhou, H., Xu, R., Zhao, Y., Chinnaswamy, K., McEachern, D., Chen, J., Yang, C.Y., Liu, Z., Wang, M. *et al.* (2019) A potent and selective small-molecule degrader of STAT3 achieves complete tumor regression in vivo. *Cancer Cell*, **36**, 498–511.
- Zengerle, M., Chan, K.H. and Ciulli, A. (2015) Selective small molecule induced degradation of the BET bromodomain protein BRD4. *ACS Chem. Biol.*, **10**, 1770–1777.
- Donovan, K.A., Ferguson, F.M., Bushman, J.W., Eleuteri, N.A., Bhunia, D., Ryu, S., Tan, L., Shi, K., Yue, H., Liu, X. *et al.* (2020) Mapping the degradable kinome provides a resource for expedited degrader development. *Cell*, **183**, 1714–1731.
- Xiang, W., Zhao, L., Han, X., Qin, C., Miao, B., McEachern, D., Wang, Y., Metwally, H., Kirchoff, P.D., Wang, L. *et al.* (2021) Discovery of ARD-2585 as an exceptionally potent and orally active PROTAC degrader of androgen receptor for the treatment of advanced prostate cancer. *J. Med. Chem.*, **64**, 13487–13509.
- Zoppi, V., Hughes, S.J., Maniaci, C., Testa, A., Gmaschitz, T., Wieshofer, C., Koegl, M., Riching, K.M., Daniels, D.L., Spallarossa, A. *et al.* (2019) Iterative design and optimization of initially inactive proteolysis targeting chimeras (PROTACs) identify VZ185 as a potent, fast, and selective von hippel-lindau (VHL) based dual degrader probe of BRD9 and BRD7. *J. Med. Chem.*, **62**, 699–726.
- Xiao, L., Parolia, A., Qiao, Y., Bawa, P., Eyunni, S., Mannan, R., Carson, S.E., Chang, Y., Wang, X., Zhang, Y. *et al.* (2022) Targeting SWI/SNF ATPases in enhancer-addicted prostate cancer. *Nature*, **601**, 434–439.
- Jiang, B., Gao, Y., Che, J., Lu, W., Kaltheuner, I.H., Dries, R., Kalocsay, M., Berberich, M.J., Jiang, J., You, I. *et al.* (2021) Discovery and resistance mechanism of a selective CDK12 degrader. *Nat. Chem. Biol.*, **17**, 675–683.
- Maple, H.J., Clayden, N., Baron, A., Stacey, C. and Felix, R. (2019) Developing degraders: principles and perspectives on design and chemical space. *Medchemcomm*, **10**, 1755–1764.
- Edmondson, S.D., Yang, B. and Fallan, C. (2019) Proteolysis targeting chimeras (PROTACs) in ‘beyond rule-of-five’ chemical space: recent progress and future challenges. *Bioorg. Med. Chem. Lett.*, **29**, 1555–1564.
- Chamberlain, P.P. and Hamann, L.G. (2019) Development of targeted protein degradation therapeutics. *Nat. Chem. Biol.*, **15**, 937–944.
- Weng, G., Li, D., Kang, Y. and Hou, T. (2021) Integrative modeling of PROTAC-Mediated ternary complexes. *J. Med. Chem.*, **64**, 16271–16281.
- Li, D., Zhou, W., Pang, J., Tang, Q., Zhong, B., Shen, C., Xiao, L. and Hou, T. (2019) A magic drug target: androgen receptor. *Med. Res. Rev.*, **39**, 1485–1514.
- Deveraux, Q.L. and Reed, J.C. (1999) IAP family proteins—suppressors of apoptosis. *Genes Dev.*, **13**, 239–252.
- Sastry, G.M., Adzhigirey, M., Day, T., Annabhimoju, R. and Sherman, W. (2013) Protein and ligand preparation: parameters, protocols, and influence on virtual screening enrichments. *J. Comput.-Aided Mol. Des.*, **27**, 221–234.
- Friesner, R.A., Banks, J.L., Murphy, R.B., Halgren, T.A., Klicic, J.J., Mainz, D.T., Repasky, M.P., Knoll, E.H., Shelley, M., Perry, J.K. *et al.* (2004) Glide: a new approach for rapid, accurate docking and scoring. 1. Method and assessment of docking accuracy. *J. Med. Chem.*, **47**, 1739–1749.
- Garzon, J.I., Lopez-Blanco, J.R., Pons, C., Kovacs, J., Abagyan, R., Fernandez-Recio, J. and Chacon, P. (2009) FRODOCK: a new approach for fast rotational protein-protein docking. *Bioinformatics*, **25**, 2544–2551.
- Gray, J.J., Moughon, S., Wang, C., Schueler-Furman, O., Kuhlman, B., Rohl, C.A. and Baker, D. (2003) Protein–Protein docking with simultaneous optimization of Rigid-body displacement and Side-chain conformations. *J. Mol. Biol.*, **331**, 281–299.
- Olechnovic, K. and Venclovas, C. (2017) VoroMQA: assessment of protein structure quality using interatomic contact areas. *Proteins*, **85**, 1131–1145.
- Rodrigues, J.P., Trellet, M., Schmitz, C., Kastritis, P., Karaca, E., Melquiond, A.S. and Bonvin, A.M. (2012) Clustering biomolecular complexes by residue contacts similarity. *Proteins*, **80**, 1810–1817.
- Rego, N. and Koes, D. (2015) 3Dmol.js: molecular visualization with WebGL. *Bioinformatics*, **31**, 1322–1324.